

Formation of Gd-Al Alloy Films by a Molten Salt Electrochemical Process

Concha Caravaca and Guadalupe De Córdoba

CIEMAT, Departamento de Energía/División de Fisión Nuclear/URAA, Avda. Complutense, 22, Madrid, 28040, Spain

Reprint requests to Dr. C. C.; Fax: +34-91-3466233; E-mail: c.caravaca@ciemat.es

Z. Naturforsch. **63a**, 98–106 (2008); received December 1, 2006

Presented at the EUCHEM Conference on Molten Salts and Ionic Liquids, Hammamet, Tunisia, September 16–22, 2006.

The electrochemistry of molten LiCl-KCl-GdCl₃ at a reactive Al electrode has been studied at 723 to 823 K. Electrochemical techniques such as cyclic voltammetry and chronopotentiometry have been used in order to identify the intermetallic compounds formed. Cyclic voltammetry showed that, while at an inert W electrode GdCl₃ is reduced to Gd metal in a single step at a potential close to the reduction of the solvent, at an Al electrode a shift towards more positive values occurs. This shift of the cathodic potential indicated a reduction of the activity of Gd in Al with respect to that of W, due to the formation of alloys. The surface characterization of samples formed by both galvanostatic and potentiostatic electrolysis has shown the presence of two intermetallic compounds: GdAl₃ and GdAl₂. Using open-circuit chronopotentiometry it has been possible to measure the potentials at which these compounds are transformed into each other. The values of these potential plateaus, once transformed into e. f. m. values, allowed to determine the thermodynamic properties of the GdAl₃ intermetallic compound.

Key words: Molten Salts; Gadolinium; Electrolysis; Alloy Formation; Pyrochemical Processes.

1. Introduction

For future innovative reactor systems an important criterion to be taken into account is the sustainability, including minimization of waste output and its radiotoxicity. The most radiotoxic actinoides (Pu, Np, Am and Cm) have a great impact, therefore their recycling is compulsory [1, 2].

Over the last few years a huge amount of research has been carried out worldwide with the aim of separating these actinoides and transmuting them, in dedicated nuclear reactors, into stable or short-lived radionuclides. Processes that are considered use both electrochemical (electrorefining and/or electrolysis) and reductive salt extraction/metal techniques. The molten salt media under study are mainly chlorides and fluorides of alkali and alkaline earth metals. Some of the advantages of these high-temperature processes are the radiation resistance of the salt and metal phases used, that allows a high actinoid content in the medium and short cooling times, and their inherent proliferation resistance.

Special attention has been paid to the separation of actinoides (An) from lanthanoides (Ln) due

to their similar chemical properties that make their separation quite difficult. Due to the neutronic poison effect of some of the lanthanoides their allowed content in future nuclear fuel has to be kept low.

For homogeneous recycling of all actinoides, pyrochemical processes involving high temperature, using molten salt and metal phases, are considered as a promising alternative to hydrometallurgical processes. Thermodynamic calculations have shown that aluminium could be a promising metallic solvent to support the grouped recovery of An with an efficient separation from Ln [3, 4]. In chloride media, the An-Ln separation is being developed using electrochemical techniques. In order to develop a future nuclear cycle, the understanding of the chemical and electrochemical behaviour of the actinoides and lanthanoides is necessary. This includes a good knowledge of both the thermodynamic and kinetic properties of the different elements contained in the spent nuclear fuel, in the salt and metal phases. Among the lanthanoides, the study of the gadolinium behaviour is interesting because of its significant content in the spent nuclear fuel and its reduction potential in molten LiCl-KCl, that is close to

those of An, which makes difficult the selective separation.

The electrochemical behaviour of Gd in LiCl-KCl at inert cathodes has already been studied at CIEMAT [5] and several other places [6–9]. The present paper is the continuation of the systematic determination of the basic properties of actinoides and fission products that is being carried out at CIEMAT within the EUROPART project of the European Commission. The present work deals with the identification and characterization of the Gd-Al intermetallic compounds in the molten eutectic LiCl-KCl, which have been carried out using the technique of open-circuit chronopotentiometry and performing electrolyses at constant potential and current at Al plates. The characterization of the alloys formed, performed by different techniques, showed the formation of the intermetallic compounds GdAl₃ and GdAl₂, depending on the potential applied. The determination of the thermodynamic properties of GdAl₃ has been performed by e. m. f. measurements. Comparison of the present results with those found in the literature [9] showed good agreement both in the thermodynamic data and also in the two intermetallics identified.

2. Experimental

Storage and handling of the chemicals was carried out in a glovebox under pure Ar(g) (Air Liquide; H₂O, < 0.5 ppm, and O₂, < 0.1 ppm). Electrochemical experiments were performed in a sealed quartz cell under Ar(g), additionally purified by passing through both a moisture and an oxygen trap (Agilent). The thermocouple and electrodes were positioned in a cell which also supported a vitreous carbon crucible (Sofacel S.A.) containing the electrolyte.

The electrolyte was the eutectic LiCl-KCl (59:41 mol%) (Aldrich, 99% – Merck, 99.999%). The preparation of LiCl-KCl was performed by heating a mixture at 200 °C under vacuum for 22 h before melting. The temperature was then raised to 450 °C under Ar(g). Once melted, the bath was purified by HCl(g) treatment (Air Liquide; H₂O, < 10 ppm) for 45–60 min, followed by Ar(g) sparging in order to remove the dissolved HCl(g).

Solutions of GdCl₃ (Aldrich, 99.99%) were prepared by direct addition of anhydrous trichlorides without further treatment.

The electrochemical study has been performed using a three electrode set-up with a potentiostat-

galvanostat Autolab PGSTAT30 (Eco-Chimie) controlled with an Autolab GPES software v.4.9.

Metallic inert tungsten (∅1 mm, Goodfellow 99.9%) and solid reactive aluminium (∅1 mm, Aldrich, 99.999%) wires, and Al plates (0.5 and 1 mm thickness, Aldrich, 99.999%) were used as working electrodes. Before the electrochemical measurements the working electrodes were rinsed with ethanol in an ultrasonic bath. The surface area of the electrodes was determined after each experiment by measuring the immersion depth into the molten salt.

The reference electrode consisted of an Ag wire (∅1 mm, Aldrich, 99.99%) dipped in a closed-end Pyrex glass tube containing a 0.75 mol kg⁻¹ AgCl (Merck, 99.4%) solution in LiCl-KCl. The counter electrodes consisted of vitreous either carbon or graphite rods (∅3 mm, Sofacel S. A.).

Gd-Al alloy samples were washed either with water and then ethanol or with a mixture of ethanol/water (80:20 vol%) in an ultrasonic bath in order to remove the residual salt before the surface analysis. This procedure has been used by Nohira et al. for Pr-Ni alloys [10], and it has been applied for Gd-Al since Colinet indicated that Gd-Al compounds, especially those rich in Al, are very stable [11].

Surface analysis of the Gd-Al alloys formed was performed by X-ray diffraction (XRD) (X'Pert, MPD Philips), using Cu as anode, in order to identify the intermetallic compounds formed during the electrolysis. Also the techniques of scanning electron microscopy (SEM) with energy dispersive X-ray (EDX) analysis incorporated (Hitachi S-2500, 30 kV) were used to determine the surface composition and the concentration profiles of Gd in the alloy layer.

The determination of the concentration was performed by taking samples of the melt diluting them in nitric acid solutions (1 vol%), and analysing them by ICP-MS.

3. Results and Discussion

According to the Gd-Al phase diagram [12] (see Fig. 1), Gd can form 5 solid intermetallic compounds with aluminium: AlGd₂, Al₂Gd₃, AlGd, Al₂Gd and Al₃Gd, at temperatures below 650 °C which is higher than the experimental temperature range used in the present work, 450–550 °C.

In order to identify the Gd-Al alloys formed at the surface, two electrochemical techniques were used:

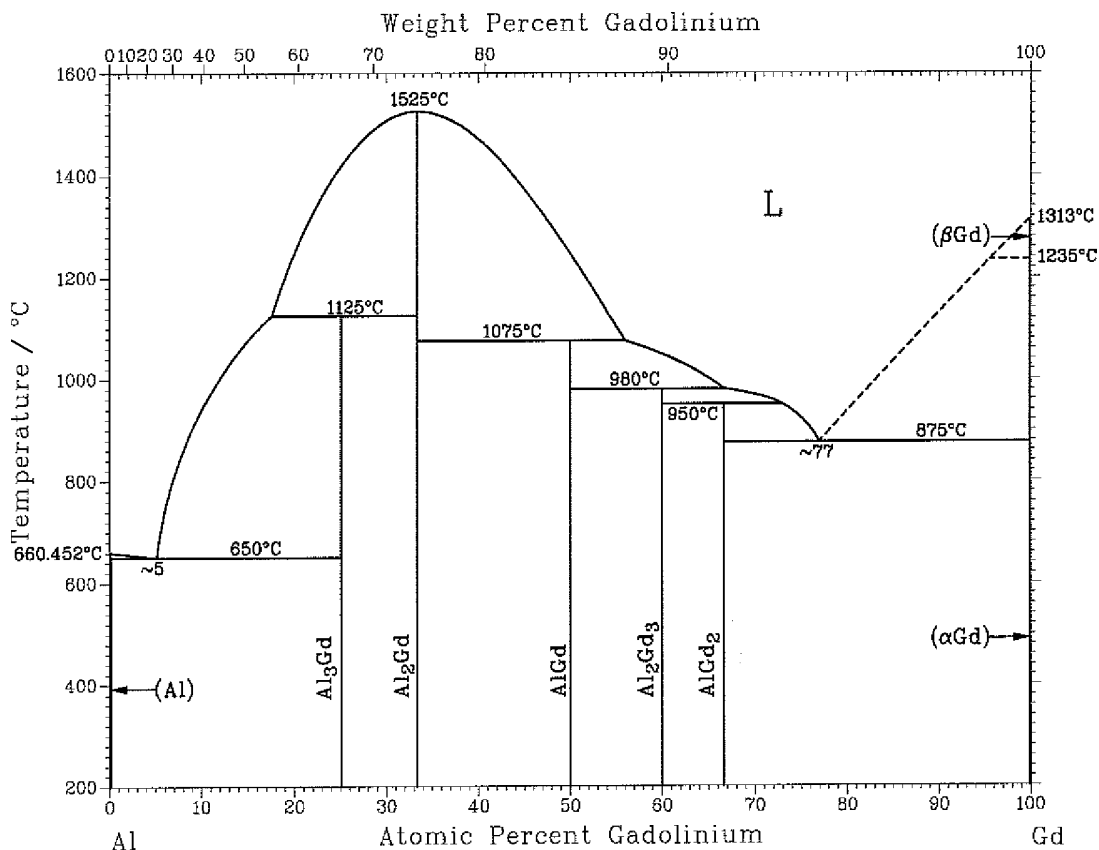


Fig. 1. Gd-Al phase diagram [12].

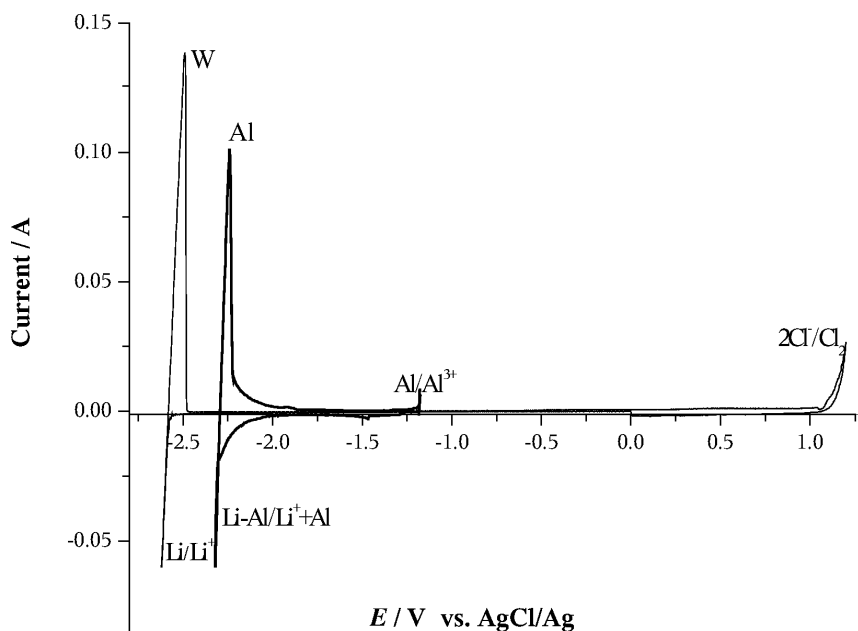


Fig. 2. Electrochemical window of the eutectic LiCl-KCl at W and Al (\varnothing 1 mm) working electrodes; temperature, 723 K; scan rate, 0.1 V s⁻¹.

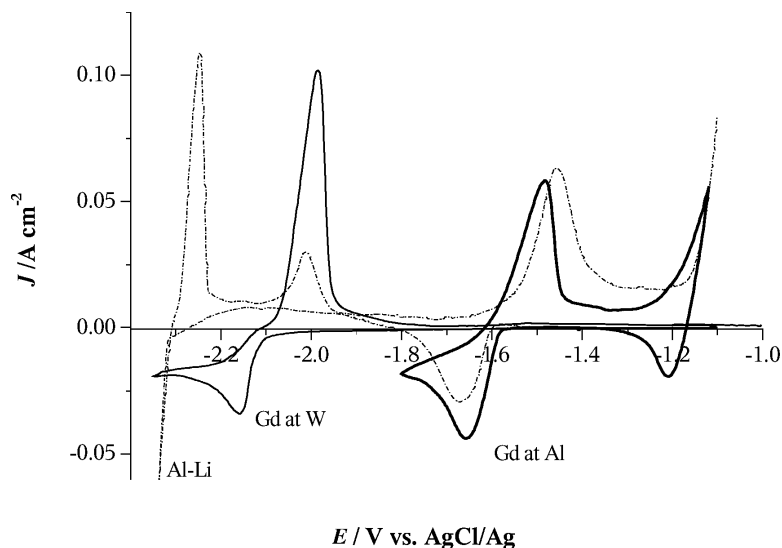


Fig. 3. Cyclic voltammogram of Gd(III) at an inert W electrode ($S = 0.22 \text{ cm}^2$) and at a reactive solid Al working electrode ($S = 0.45 \text{ cm}^2$); Gd^{3+} concentration, $6.0 \cdot 10^{-2} \text{ mol kg}^{-1}$; temperature, 733 K; scan rate, 0.1 V s^{-1} .

open-circuit potentiometry (OCP) and cyclic voltammetry (CV). A GdCl_3 solution of $6.0 \cdot 10^{-2} \text{ mol kg}^{-1}$ was used in the determination of equilibrium potentials of coexisting phases.

3.1. Cyclic Voltammetry

Figure 2 shows the electrochemical window of LiCl-KCl at 723 K at both W and Al electrodes. The cathodic limit that corresponds to the Li(I) reduction at the W working electrode is $-2.58 \text{ V vs. AgCl/Ag}$, whereas at the Al electrode the cathodic limit is the formation of the Li-Al alloy at $\sim -2.29 \text{ V vs. AgCl/Ag}$. A shift of the potential in the positive direction is observed when Al is used due to a decrease of the activity of Li(I) in Al as a consequence of the alloy formation.

The Gd-Al alloy formation was studied using the CV technique. A typical voltammogram of Gd^{3+} in LiCl-KCl at an inert W working electrode is shown in Figure 3. The shape of the re-oxidation peak is characteristic for the deposition of a solid compound. The voltammogram also shows that the electrodeposition of Gd^{3+} on Gd metal requires to apply an overpotential, indicating that the process is affected by a nucleation phenomenon. This nucleation phenomenon has also been corroborated by the technique of chronoamperometry.

A voltammogram of Gd at a reactive Al electrode is also shown in Fig. 3; in this case, the electrodeposition occurs at a more positive potential. This potential shift, about 0.56 V, is associated with a decrease of the

activity of Gd in Al with respect to the activity of Gd at W, produced by the formation of Gd-Al alloys. The current of this peak is associated with a reaction of the following kind [13]:



where x can take values given by the binary Gd-Al diagram of Figure 1.

No more peaks, neither cathodic nor anodic, have been observed when cyclic voltammograms were performed towards more negative potential values, as can be seen in Figure 3. The fact that the number of anodic peaks is smaller than the number of alloys in the Gd-Al phase diagram suggests that some of the reactions are very slow [10].

3.2. Open-Circuit Chronopotentiometry

Cyclic voltammetry can not be used to identify the intermetallic compounds, however, this is possible with the open-circuit chronopotentiometry technique. By this technique, after a short cathodic polarization (30–120 s) at potentials corresponding to the Gd metal electrodeposition, the open-circuit potential of the Al electrode is recorded versus time.

During the polarization, the Gd metal deposited reacts with the Al electrode surface and diffuses in its bulk. The surface composition varies from pure Gd metal to an alloy very rich in Al, thus a gradual shift of the potential towards more positive values takes place

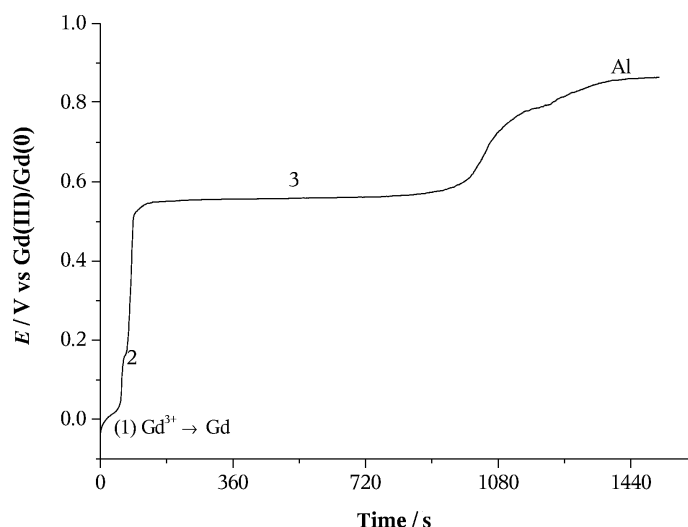


Fig. 4. Open-circuit chronopotentiogram of the LiCl-KCl-GdCl₃ system at an Al electrode at 723 K; counter electrode, vitreous carbon rod (\varnothing 3 mm); polarization time, 30 s; E_{app} , -2.135 V vs. AgCl/Ag.

[14, 15]. During this process, the curve presents potential plateaus corresponding to compositions of the electrode in which there is co-existence of two different phases.

The potential of these plateaus is given by the difference of the activity of Gd in the electrolyte, that is constant, and at the Gd-Al alloy surface, which is variable. As Gd diffuses into Al its concentration decreases at the electrode surface and the potential becomes more positive. When a two-phase equilibrium in the solid state exists at the surface of the electrode, the Gd activity is equal in each phase and remains constant while the Gd concentration decreases at the surface. This results in a constant potential plateau for a given diffusion time [13].

Figure 4 shows a potential-time curve obtained at 723 K for a molten bath containing Gd(III) at a concentration of $6.12 \cdot 10^{-2} \text{ mol kg}^{-1}$. In this figure, three plateaus are observed before the abandon potential of Al [around 0.86 V vs. Gd(III)/Gd(0)]. The first plateau corresponds to the Gd metal electrodeposition. A second plateau appears at about 0.16 V and a third plateau at around 0.56 V, both vs. Gd(III)/Gd(0).

It has been observed that the potential of the second plateau depends on the polarization time and also on the pre-electrolysis potential applied. To study the latter effect, polarization at different potentials were tested. It has been observed that, if the pre-electrolysis is performed at potentials slightly more positive than the potential of Gd metal electrodeposition, the second plateau is not observed and only the plateau at about 0.56 V appears. This behaviour and the fact of

the short length of the second plateau would indicate that the corresponding transformation reaction of one compound into the other is relatively slow [10]. Due to the difficulties of measuring the second plateau of Fig. 4, it was not taken into account for the thermodynamic properties determination; therefore only potentials corresponding to plateau 3 are going to be considered.

3.3. Gd-Al Alloy Formation by Electrolysis

In order to identify the composition of the different plateaus, potentiostatic electrolyses at values corresponding to potentials between the plateaus were performed at 450 °C. Afterwards, the deposits were analyzed by XRD, EDX and SEM techniques. Al plates of 1 mm thickness were used in all the electrolyses. The potentials selected were: -1.8 V (for 3 and 12 h), -2.0 V (for 2.5 and 3.5 h) and -2.2 V (for 2.5 and 3 h); potential values were referred vs. AgCl/Ag. These values correspond to about 0.255, 0.055 and -0.156 V vs. Gd(III)/Gd(0) at 450 °C.

The diffractograms of the samples electrodeposited at -1.80 V vs. AgCl/Ag, shown in Fig. 5a, indicate that the alloy formed consists of GdAl₃, and that the deposit shows good crystallinity. Therefore, plateau 3 is identified as the following equilibrium [16]:



Diffractograms of the samples obtained by electrolysis performed at -2.0 V vs. AgCl/Ag, see Fig. 5b,

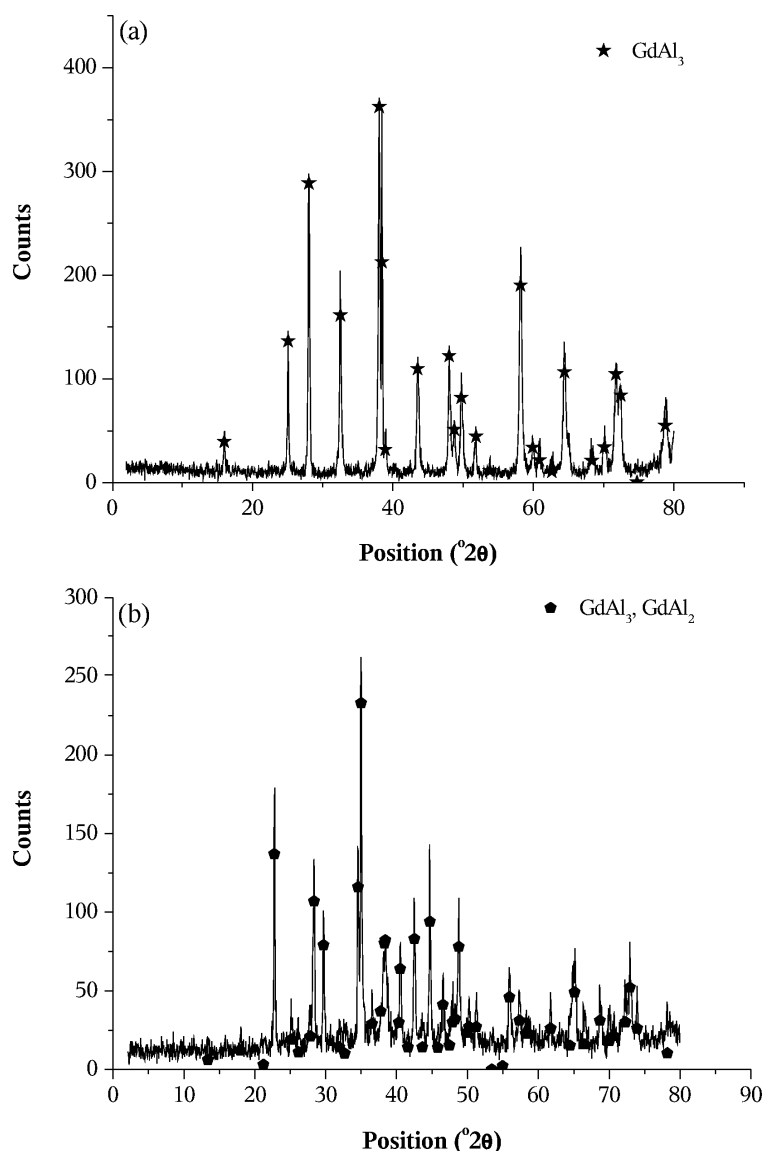
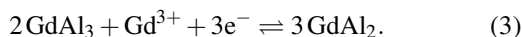


Fig. 5. (a) Diffractogram of a sample obtained by electrolysis at -1.8 V vs. AgCl/Ag for 7 h, corresponding to the GdAl_3 intermetallic compound. (b) Diffractogram of a sample obtained by electrolysis at -2.0 V vs. AgCl/Ag for 2.5 h at 723 K, consisting of GdAl_3 and GdAl_2 .

indicate the presence of the intermetallic compounds GdAl_3 as main compound and GdAl_2 as minor compound. Besides these two compounds, the presence of LiCl, KCl and GdOCl is also observed in some of the samples. The presence of GdOCl is thought to be caused by the reaction of Gd metal deposited or some GdCl_3 embedded in the salt with water during the sample washing.

Therefore, the equilibrium corresponding to plateau 2 is



For electrolyses performed at -2.2 V vs. AgCl/Ag, the compounds identified by XRD consist of GdAl_3 and GdAl_2 . For this potential, the diffractograms obtained indicate that in this case GdAl_2 is the main compound whereas GdAl_3 is the minor compound.

It has been observed that after the electrolyses at the two more negative potentials, the Al plate was covered by a black mud that partly felt down when the sample was lifted up from the salt, and the rest disappeared during washing, settling at the bottom of the beaker as a black powder. Samples obtained at -2.2 V presented a bigger black deposit. It is thought that the deposits

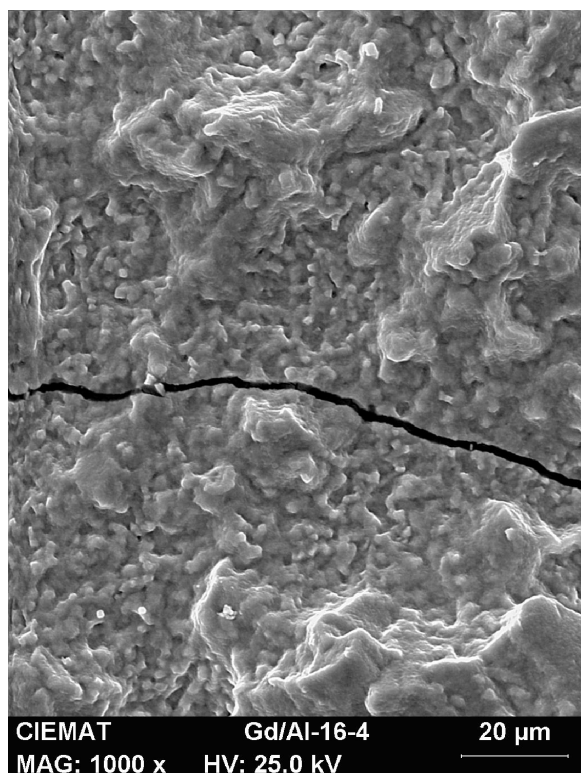


Fig. 6. Morphology of a deposit obtained by electrolysis at -1.64 V vs. AgCl/Ag at an Al plate for 7 h at 450 °C in LiCl-KCl.

could consist of some electrodeposited Li metal at the electrode surface.

Figure 6 shows the morphology of the surface of $GdAl_3$, formed by potentiostatic electrolysis at -1.64 V vs. AgCl/Ag during 7 h, obtained by SEM. The deposit is quite compact, although in the photograph it is possible to observe cracks. The compactness of the deposit can be appreciated more clearly in the cross-section of Figure 7. A quite homogeneous layer is observed along the surface of the Al plate, except for the edges, at which the thickness is slightly bigger. This edge effect is explained by a higher current flux than at the Al plate surface [17].

The corresponding surface composition obtained by EDX analysis indicates an average atomic composition of 73.11% of Al and 26.89% of Gd which agrees with the intermetallic, $GdAl_3$, observed by XRD.

During the constant current electrolysis performed at 723 K, the potential of the cathode and anode was recorded. The anodic potential was about 1.06 V vs. AgCl/Ag, that corresponds to $Cl_2(g)$ production. The chosen current values were low (5–15 mA), in or-

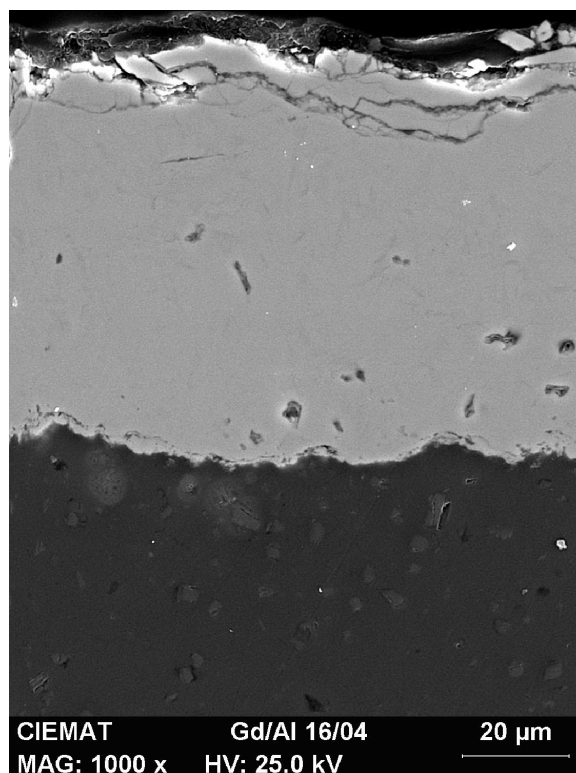


Fig. 7. Cross-section of a sample obtained by electrolysis at -1.64 V vs. AgCl/Ag for 7 h at an Al plate of 1 mm thickness, at 450 °C. The average thickness of the compact layer obtained was 80 μm.

der to obtain cathodic potential values around the half peak potential value, $E_{p/2}$, of the corresponding CV, and to avoid mass transport control. Under these conditions, only the $GdAl_3$ intermetallic compound was identified by XRD. Preliminary cross-section measurements, performed by optical microscopy, indicated that galvanostatic electrolyses yield to thicker alloy layers than potentiostatic ones for similar times.

3.4. Thermodynamic Property Determination

If the potential plateau measured from the open-circuit potentiograms is expressed vs. the Gd(III)/Gd(0) potential, the potential directly corresponds to an e. m. f. value for the two coexisting phases [14]. From these e. m. f. values several thermodynamic properties can be determined.

The Gd(III)/Gd(0) potential was determined by open-circuit chronopotentiometry, first at a W electrode and then at Al electrodes. Polarizations were performed at a potential corresponding to the Gd elec-

Table 1. Thermodynamic properties of Gd in a Gd-Al intermetallic compound in the two coexisting phases of GdAl₃ and Al.

T/K	E/V vs. Gd^{3+}/Gd^0	E/V vs. Gd^{3+}/Gd^0 [9]	$\Delta\tilde{G}_{Gd}/kJ\ mol^{-1}$	$\Delta\tilde{G}_{Gd}/kJ\ mol^{-1}\ at^{-1}$	a_{Gd}
723	0.562 ± 0.003	0.559 ± 0.004	-162.53 ± 0.87	-40.63 ± 0.22	$(1.81 \pm 0.79) \cdot 10^{-12}$
748	0.559 ± 0.004	0.556 ± 0.002	-161.83 ± 2.03	-40.46 ± 0.51	$(5.00 \pm 0.60) \cdot 10^{-12}$
773	0.557 ± 0.002	0.552 ± 0.004	-161.31 ± 0.58	-40.33 ± 0.14	$(1.26 \pm 0.87) \cdot 10^{-11}$
798	0.555 ± 0.003	–	-160.59 ± 0.87	-40.15 ± 0.22	$(3.08 \pm 0.82) \cdot 10^{-11}$
823	0.553 ± 0.002	0.546 ± 0.002	-160.06 ± 0.29	-40.02 ± 0.07	$(6.73 \pm 0.94) \cdot 10^{-11}$

trodeposition. Then, potential values corresponding to the plateau 3 were measured vs. Gd(III)/Gd(0), repeatedly in order to confirm the reproducibility. The corresponding average values obtained in this work are indicated in Table 1, for temperatures of 723–823 K, along with data found in the literature [9]. Discrepancies of potential values between our data and those of Bermejo et al. [9] vary from 3 to 7 mV (0.5–1.2%), thus indicating a good agreement.

The relative molar partial Gibbs free energy of Gd in the GdAl₃ intermetallic compound in two coexisting states, $\Delta\tilde{G}_{Gd}$, was calculated from the e. m. f. measurements [E/V vs. Gd(III)/Gd(0)], corresponding to the plateau 3, by the equation [14]

$$\Delta\tilde{G}_{Gd} = -3F\Delta E. \quad (4)$$

Thermodynamic data estimated this way are shown in Table 1. The relative molar enthalpy and entropy of Gd were also calculated from the Gibbs-Helmholtz equation. The expression obtained for this temperature dependence is

$$\Delta\tilde{G} = -180.48(\pm 1.64) + 0.0249(\pm 0.0011)T \quad (5)$$

$(T/K).$

The e. m. f. corresponding to the alloy formed at the electrode surface is related to the activity of Gd by the following expression [14, 15]:

$$\Delta E = \text{e. m. f.} = -\frac{RT}{nF} \ln a_{Gd}, \quad (6)$$

where a_{Gd} is the activity of Gd in the alloy (Al). Values obtained with this expression are also given in Table 1. The obtained activity values indicate a low solubility of Gd in Al.

The values of the relative molar partial Gibbs free energy of Gd in the Gd-Al intermetallic compound and the activity determined in this work agree well with those found in the literature [9].

4. Conclusions

Electrochemical transient techniques, such as cyclic voltammetry and chronopotentiometry, have been used to identify the Gd-Al intermetallic compound formation in LiCl-KCl. The open-circuit potentiometry technique has also allowed to measure the e. m. f. values from the potential-time plateaus in order to determine the thermodynamic properties of two coexisting phases.

The two Gd-Al intermetallic compounds, identified by the surface analysis of the deposit formed by electrolysis at potential values between successive plateaus, were GdAl₃ and GdAl₂. The Al richer compound showed higher stability, longer plateau, which is in agreement with the literature reviewed. Due to the inaccuracy of potential values corresponding to the state of GdAl₂+GdAl₃ coexistence, thermodynamic properties have only been estimated for the GdAl₃ intermetallic compound in the temperature range 723–823 K.

Acknowledgements

This work is part of a project performed at CIEMAT within the WP6 of the EUROPART project of the European Commission. The authors thank ENRESA for financial support within the agreement CIEMAT-ENRESA, Annex X, about separation of long living radionuclides, No. 7800087. The authors also thank L. Gutiérrez, A. M. Lancha, A. del Rio, J. Quiñones, M. J. Tomás and M. Rosado for technical assistance.

[1] OCDE/NEA, Actinide and Fission Product Partitioning and Transmutation. Status and Assessment Report, OCDE Nuclear Agency, Paris 1999, pp. 27–68.

[2] OCDE/NEA, Accelerator-Driven Systems (ADS) and Fast Reactors (FR) in Advanced Nuclear Fuel Cycles. A Comparative Study, OCDE Nuclear Agency, Paris 2002, pp. 15–23.

- [3] V.A. Lebedev, *Selectivity of Liquid Metal Electrodes in Molten Halides*, Metallurgiya, Chelyabinsk, Moscow 1993 (in Russian and English translation).
- [4] J. Serp, R. Malmbeck, and J.-P. Glatz, 7th International Symposium on Molten Salts Chemistry & Technology, Toulouse, France, 29 August – 2 September 2005, p. 577.
- [5] C. Caravaca, G. de Córdoba, M.J. Tomas, and M. Rosada, *J. Nucl. Mater.* **360**, 25 (2007).
- [6] F. Lantelme and Y. Berghoute, *J. Electrochem. Soc.* **146**, 4137 (1999).
- [7] S.P. Fusselman, J.J. Roy, D.L. Grimmett, L.F. Grantham, C.L. Krueger, C.R. Nabelek, T.S. Storvick, I. Tadashi, H. Takatoshi, K. Kensuke, S. Yoshiharu, U. Koichi, K. Tsutomu, and T. Noriaki, *J. Electrochem. Soc.* **146**, 2573 (1999).
- [8] J.J. Roy, L.F. Grantham, L.R. McCoy, C.L. Krueger, T.S. Storvic, T. Inoue, H. Miyashiro, and N. Takahashi, *Mater. Sci. Forum* **73 – 75**, 547 (1991).
- [9] M.R. Bermejo, J. Gomez, J. Medina, A.M. Martinez, and Y. Castrillejo, *J. Electroanal. Chem.* **588**, 253 (2006).
- [10] T. Nohiro, H. Kambara, K. Amezawa, and Y. Ito, *J. Electrochem. Soc.* **152**, C183 (2005).
- [11] C. Colinet, A. Pasturel, and K.H.J. Buschow, *Physica B+C* **150**, 397 (1988).
- [12] K.A. Gschneidner and F.W. Calderwood, *Bull. Alloy Phase Diagrams* **9**, 6 (1988).
- [13] L. Massot, P. Chamelot, and P. Taxil, *Electrochim. Acta* **50**, 5510 (2005).
- [14] H. Konishi, T. Nishikiori, T. Nohira, and Y. Ito, *Electrochim. Acta* **48**, 1403 (2003).
- [15] G.D. Picard, Y.E. Mottot, and B.L. Trémillon, *Proc. Electrochem. Soc.* **84**, 585 (1984).
- [16] P. Taxil, *J. Less-Common Met.* **113**, 89 (1985).
- [17] D. Pletcher, Lecture 7. Potential and current distributions in electrochemical cells. Summer School on Electrochemistry, Electrochemical Engineering and Electrochemical Technology, Southampton University, UK 2006.